APPLE UNDULATOR FOR PETRA III

J. Bahrdt, H.-J. Baecker, W. Frentrup, A. Gaupp, M. Scheer, B. Schulz, BESSY, Berlin, Germany,
U. Englisch, M. Tischer, DESY, Hamburg, Germany

Abstract

Currently, the storage ring PETRA is being rebuilt to a light source with an ultra low emittance. The undulator radiation will take full advantage of this high performance. Within the energy range of 250–3000eV an APPLE II type undulator will provide light with arbitrary polarization. This APPLE II undulator is under construction at BESSY. Results of the detailed magnet block characterization including block inhomogeneities are presented. The total length of 5m and a minimum gap of only 11mm cause strong 3D forces which require a sophisticated mechanical layout. The mechanical concept and the expected deformations are presented.

INTRODUCTION

The 6GeV storage ring PETRA III [1, 2] will have an emittance of 1nmrad which is accomplished by damping wigglers with a total length of 80m [3]. One octant of the ring is completely rebuilt in order to include up to 14 undulators [4]. Most of the insertion devices produce linearly polarized light. An APPLE II undulator will deliver light with variable polarization in the range of 250-3000eV. This device which is currently built at BESSY is similar to the BESSY UE112 APPLE undulator design [5], though the strong 3D-forces in the inclined mode require several modifications.

SPECTRAL PERFORMANCE

The undulator parameters are driven by the demand to cover the complete energy regime with the first harmonic. This guarantees nearly 100% degree of circular polarization and high photon fluxes. The row phases for the circular mode and the 45° inclined mode vary slightly with the magnetic gap (figure 1) due to the different gap dependence of horizontal and vertical fields.

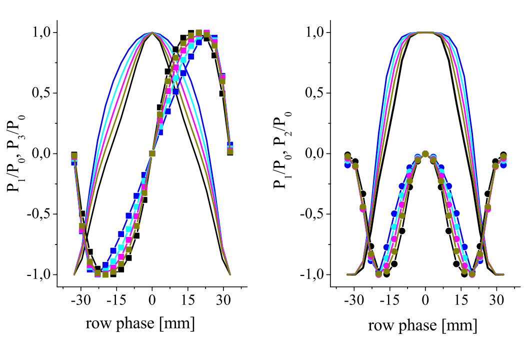

Figure 1: Simulated degree of polarization in the elliptical (left) and inclined mode (right) at gaps of 11 (black), 19 (green), 27 (magenta), 35 (light blue) and 45 mm (dark blue). No symbols: P_1 / P_0, with symbols: $P_{2(3)} / P_0$.

With a minimum magnetic gap of 11mm the period length is 65.6mm. The minimum photon energies for the different operation modes are given in table 1.

Table 1: UE65-parameters calculated for minimum gap.

operation mode	row phase [mm]	effective field [Tesla]	1st harmonic [eV]
hor. linear	0	1.147	204
vert. linear	32.80	0.985	274
circular	18.10	1.068	234
inclined 45°	17.35	0.760	444

MAGNET MATERIAL

Both magnet types, the longitudinally magnetized A-magnets and the vertically magnetized B-magnets, are dye pressed. The magnets have different grades with: $B_{r,\,min}$ / $H_{cj,\,min}$ = 1.28 T / 1670 kA/m (type A) and 1.33 T / 1275 kA/m (type B). The blocks have been magnetized in two different orientations related to the pressing geometry (AN/AS and BN/BS) to allow for a compensation of systematic effects [6]. All magnets were measured in an automated Helmholtz coil and, additionally, with a stretched wire system which delivers information on the block inhonmogeneity [5-7]. The wire data haven been taken at all relevant sides (A-magnets: four sides, B-magnets: 2 sides). Two dipole components have been fitted to the difference of two wire measurements at opposite magnet sides. The difference spectrum adds the dipole contributions and cancels the higher order multipole components with identical sign and shape at opposite sides. Remaining inghomogeneities contribute to the residuals of the fit. The fitted dipoles show a good correlation with the Helmholtz coil data (figure 2).

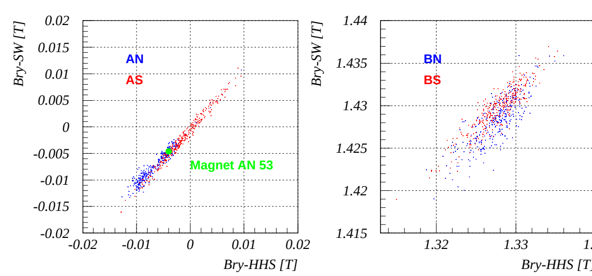

Figure 2: Correlation of the vertical dipole component as measured with the Helmholtz coil (HHS) and the stretched wire system (SW), respectively.

The widths of the correlation plots indicate the limited accuracy of the stretched wire system for dipole measurements as compared to the Helmholtz coil system. The larger deviation for the B-magnets is partly due to the higher positioning sensitivity of the measurement system if the main dipole component points perpendicular to the wire. The inhomogeneities as measured with the stretched wire contribute significantly to the field integrals even at large gaps (figure 3).

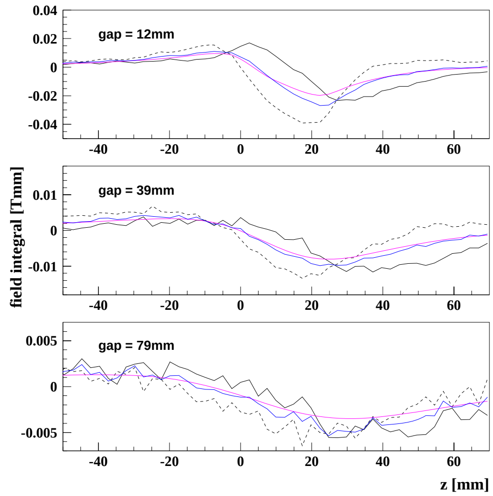

Figure 3: Transverse distribution of vertical field integrals measured at two opposite sides of magnet AN 53 (black solid and black dashed (sign reversed)). The average (blue) reproduces the data extrapolated from dipole data (magenta) as measured with the Helmholtz coil.

A statistical analysis demonstrates that the field integral contributions from the dipole moments alone and from the inhomogeneities (dipole contributions are subtracted) have roughly the same strength (figures 4 and 5). It is essential to use both data sets for an effective sorting and a reliable prediction of the undulator performance [5].

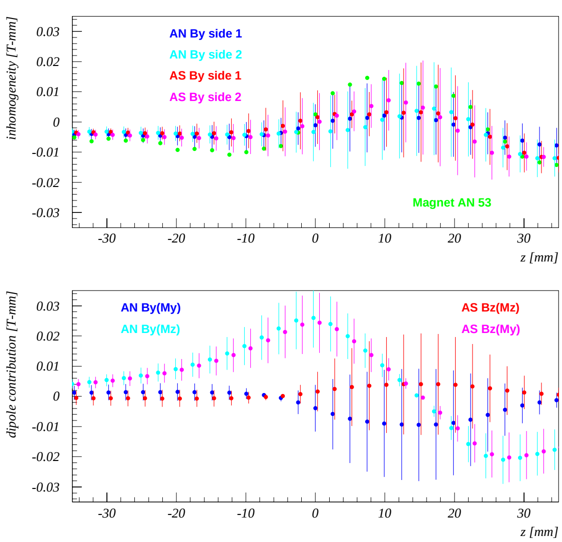

Figure 4: Field integrals averaged over all A-magnets of one type originating from the block inhomogeneities alone, excluding the dipole components (top) and by the dipole components alone (bottom). The error bars indicate twice the rms value of the distribution at each z-value. The green curve represents the individual data of magnet AN 53 (see figure 3).

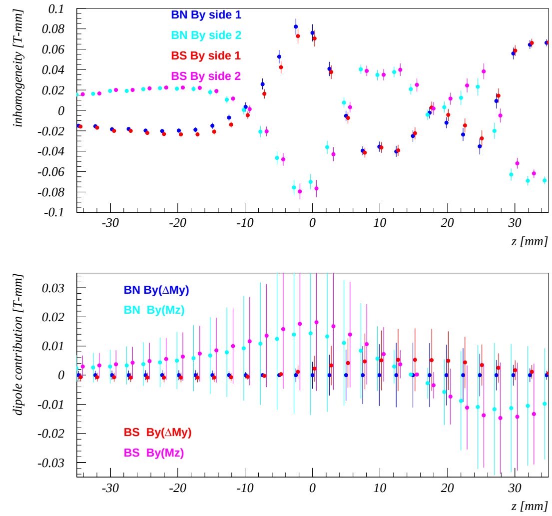

Figure 5: Field integrals averaged over all B-magnets of one type originating from inhomogeneities alone, excluding the dipole components (top) and by the dipole components alone (bottom). See also figure caption 4.

MECHANICAL LAYOUT

The UE65 forces and torques are about a factor of two higher as compared to the BESSY UE112 (table 2). The support structure is made from a single piece of cast iron (figure 6). The Al-girders for the magnetic structure are milled from solid blocks in order to avoid the welding of aluminium. The magnet girders are supported at four locations using two cross bars inside each of the girders to minimize the deflection under magnet load. The residual bending is only ±2μm.

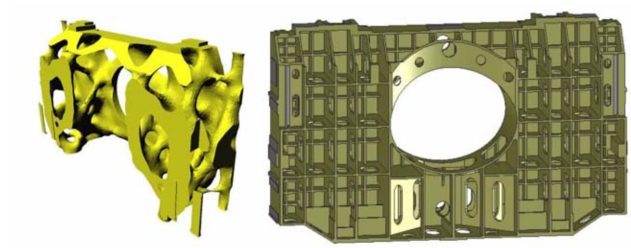

Figure 6: Cast iron support structure: result from bionic optimization (left) and final shape (right).

Without any compensation the girders would tilt in the inclined mode by about 168μrad which would cause an unacceptable increase of the minimum gap of 0.84mm. Therefore, four instead of two servo motors are used: two motors which are moving the lower girder are controlled by two linear encoders mounted to the stiff support structure. The other two motors move the upper girder and use the gap measurement system [8] for the feed back loop.

Each magnet girder is attached to the support structure with four transverse flexible joints and one longitudinal flexible joint. These joints have been optimized for a maximum stiffness in one specific direction (transversally or longitudinally) and a minimum stiffness in another direction allowing for a girder tapering and thermal expansions without generating additional strong forces or torques (figure 7).

All four magnet rows can be moved which permits a rotation of the linear polarization vector in the inclined mode by 180°. Due to the large longitudinal force on the magnet rows of up to 58kN the rows are split longitudinally and each subassembly is driven by an individual screw. Both screws are connected to a common motor via a gear box (figure 8).

Table 2: Magnetic forces and torques (F_i and T_i) on one magnet girder for row phase = 0mm and for the inclined mode with row phase = 16.4mm. The coordinates are given in figure 8. The reference points for T_x and T_z are the centre between the two transverse flexible joints (T_x) and the longitudinal flexible joint (T_z), respectively.

units: kN, kNm	F_x	F_y	F_z	T_x	T_y	T_z
hor. linear	0	73	0	0	0	0
inclined, 16.4 mm	54	≈ 0	12	6.4	0.75	22.5

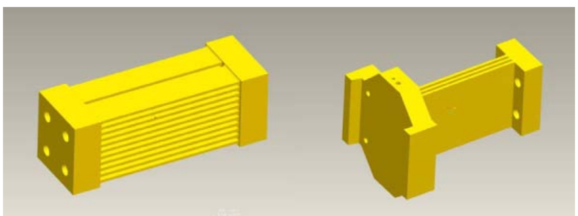

Figure 7: Flexible joints for transverse (right) and longitudinal (left) guiding of the magnet girder.

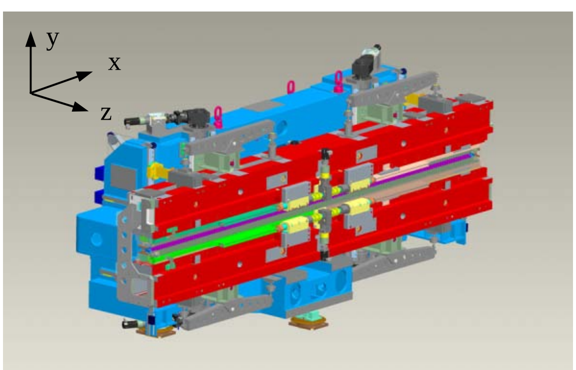

Figure 8: Mechanical Layout of the UE65.

The displacements and rotations of the two magnet girders can be separated into parallel and opposite movements (figure 9). These movements have different influences on the performance of the undulator [5].

The expected girder movements are summarized in table 3. They cause systematic field variations over the length of the undulator. The field variations perpendicular to the undulator axis depend quadratically on y and z :

$$\Delta B_{eff} / B_{eff} = a_{y(z)} \cdot y(z)^2 \qquad \text{eq. 1}$$

where the coefficients $a_{y(z)}$ are given in table 4.

The field variations are small and will not degrade the spectral performance of the undulator. These data may even be acceptable for FEL applications which require tighter tolerances on B-field variations. This topic is subject to further investigations.

Table 3: Calculated movements of the two magnet girders under maximum load in inclined mode. The relative displacements Δx_1, Δy_1, Δz_1 and relative angles $2\theta_1$, $2\varphi_1$, $2\delta_1$ are given. The red numbers are achievable only with the described feedback systems.

units: µm, µrad	fig. 8	x / δ	y / φ	z / θ
same displacement	b	12	**4**	5
opposite displacement	a	257	**1**	30
same rotation	d	100	17	**7**
opposite rotation	c	20	10	**0.4**

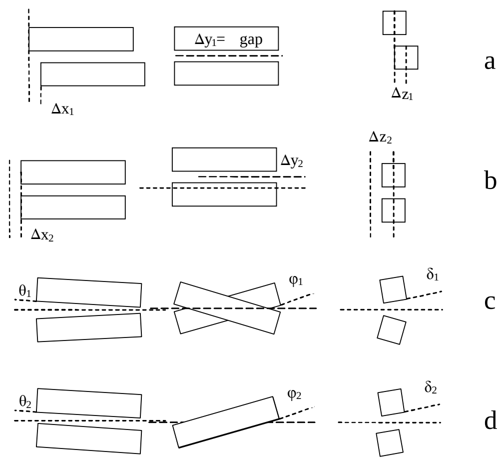

Figure 9: Girder misalignment.

Table 4: Scaling factors for evaluating the transverse field variations of the UE65 at smallest gap of 11mm (eq. 1).

operation mode	a_y [0.001/mm**2]	a_z [0.001/mm**2]
hor. linear	2.0	0.4
circular	4.6	11.5
vert. linear	12.7	16.9
inclined 45°	5.1	8.6

REFERENCES

[1] PETRA III Technical Design Report, DESY 2004-035; http://petra3.desy.de.
[2] K. Balewski, these proceedings.
[3] M. Tischer et al., Proceedings of the EPAC, Edinburgh, Scotland, 2006, pp 3565 3567.
[4] M. Tischer et al., AIP Proceedings of the Synchrotron Radiation Conference, Daegu, South Korea, 2006, pp 343-346.
[5] J. Bahrdt, Proceedings of the FEL-conference, Berlin, Germany, 2006, pp 521-528.
[6] J. Bahrdt et al., Nucl. Instr. and Meth. in Phys. Res. A, 516 (2004) 575-585.
[7] F.-J. Boergermann et al., these proceedings.
[8] J. Bahrdt et al., Proceedings of the FEL Conference 2004, Trieste, Italy, pp 610-613.